Hindawi Publishing Corporation
International Journal of Antennas and Propagation
Volume 2013, Article ID 705087, 8 pages
http://dx.doi.org/10.1155/2013/705087

Research Article

Simultaneous Altitude and RCS Estimation with Propagation Attenuation in Bistatic HFSWR

Zhao Kongrui, Yu Changjun, Zhou Gongjian, and Quan Taifan

Department of Electronic Engineering, Harbin Institute of Technology, Harbin 150001, China

Correspondence should be addressed to Yu Changjun; yuchangjun@hit.edu.cn and Zhou Gongjian; krzhao@126.com

Received 30 May 2013; Revised 29 September 2013; Accepted 13 October 2013

Academic Editor: Atsushi Mase

High frequency surface wave radar (HFSWR) is traditionally unable to detect target altitude information. To simultaneously estimate the target altitude and radar cross-sections (RCS) with bistatic T/R-R HFSWR, a novel estimation model is proposed with the variation of the propagation attenuation, and the target echoes are utilized to construct the measurement equation. The presented model is completely observable to the target state, which can contribute to preferable estimation results. In order to improve the estimation accuracy, a centralized fusion model is adopted to fuse four measurement vectors. Simulations and practical examples demonstrate the effectiveness of the proposed estimation model.

1. Introduction

High frequency surface wave radar (HFSWR) transmits vertically polarized electromagnetic waves to track ships and aircrafts at ranges of several hundreds of kilometers [1, 2]. It has been extensively applied to exclusive economic zone surveillance [3, 4] and remote sensing [5–8]. The use of the frequencies makes it difficult to form a narrow beam on elevation; HFSWR is traditionally unable to detect the target altitude information.

Many altitude estimation methods have been proposed for monostatic radar. However, all of these models are low observable; the incorrect initial altitude value would lead to large estimation errors. In order to eliminate this drawback, [9] proposed an autonomous multiple model method named Height-parameterized extended kalman filter (HPEKF) for 3D tracking with monostatic 2D radar. It was inspired by the range-parameterized EKF in bearing only tracking. In HPEKF, the main idea is that the altitude interval of interest is divided into a number of subintervals, and each subinterval deals with an independent EKF. The target state and covariance are obtained by performing weighted sum of individual estimates and covariance matrix, respectively. It means that the initial state is represented by a Gaussian mixture, each mixture component is initialized by an assumed initial altitude and tracked with an EKF. It is worthwhile to note that some of the EKFs will lead to divergence without mixture step between the independent components. In order to alleviate the drawbacks of the incorrect initialization, an initial altitude estimator with Newton iteration method was presented [10], which assumes that the aircraft flies with nearly constant velocity and altitude, and it hardly meets the real flying situation. This method can provide an accurate initial state when the measurement errors are small. Nevertheless, it is sensitive to the measurement errors, which will lead to worse results in HFSWR. An extend Kalman filter (EKF) method was proposed to estimate the altitude and RCS real time in [11]; the measurement equation is constructed with the target echo amplitude, which is the function of altitude and RCS. This model has several serious flaws; it is low observable and sensitive to the initial state. The filter would lead to divergence if the model is initialized with large error.

Multilateration method and maximum likelihood estimation are two common approaches to estimate target altitude in bistatic radar system [12, 13]. Although multilateration method is intuitive to compute the altitude of aircraft, the result usually fluctuates intensely. Maximum likelihood estimation could reach a theoretical optimal solution; the flaw is that it converges slowly and cannot provide a global optimum in most cases. Besides, these prevailing methods could not provide an approach to estimate the radar cross-section (RCS) of aircraft.

The RCS of aircraft is also essential to the target classification. Little attention has been paid to the RCS estimation in HFSWR field. Current aircraft tracking methods are mainly based on range, azimuth, and radial velocity information; it is hardly able to extract the aircraft RCS without incorporating the target echo information and propagation attenuation of ground wave. The target echoes can be represented as the function of propagation attenuation and RCS, and there are different propagation attenuations at corresponding altitudes. The two properties could provide an altitude and RCS estimation capability.

In this paper, a simultaneous altitude and target RCS estimation model is proposed through the variance of propagation attenuation. The amplitude of target echoes is utilized to construct the measurement equation, which is the nonlinear function of the altitude and RCS. Four measurement vectors are established with range, azimuth, and echo amplitude. Centralized fusion EKF model is adopted to further improve the estimation performance. Monte Carlo simulations illustrate the effectiveness and benefits of this proposed model.

The rest of the paper is presented as follows. Section 2 analyzes the relation between ground wave propagation attenuation and target altitude. A simultaneous altitude and RCS estimation model is described with centralized fusion estimation model in Section 3. In Section 4, Monte Carlo simulations and practical examples are performed to demonstrate the benefits of the proposed estimation model. Section 5 concludes the paper.

2. HF Ground Wave Propagation Attenuation

From T/R-R HFSWR equation, the echo amplitude corresponding to T/R station can be defined as

$$P_{tr} = P_t G_t \frac{1}{l_b^2(R_t, h)} \frac{\sigma_t}{(\lambda^2/4\pi)} G_r, \tag{1}$$

where P_t is the transmitted signal amplitude and G_t and G_r are the gains of transmitter and receiver, respectively. $l_b(\cdot)$ represents the ground wave propagation attenuation, R_t is the target range to T/R station, and h denotes the target altitude. The wavelength of HFSWR is λ, and σ_t is the target RCS corresponding to T/R station. Equation (1) in log can be expressed as

$$P_{tr}\,(\mathrm{dB}) = -20\log\left(l_b(R_t, h)\right) + 10\log(\sigma_t) + 10\log(C), \tag{2}$$

where

$$C = P_t G_t \frac{G_r}{(\lambda^2/4\pi)}. \tag{3}$$

If the radar parameters are fixed, C represents a constant.

The echo amplitude corresponding to R station is presented as

$$P_{rr} = P_t G_t \frac{1}{l_b(R_t, h)} \frac{\sigma_r}{(\lambda^2/4\pi)} \frac{1}{l_b(\rho - R_t, h)} G_r, \tag{4}$$

where σ_r and ρ are the RCS and the range sum corresponding to R station, respectively. Equation (4) in log can be expressed as

$$\begin{aligned} P_{rr}\,(\mathrm{dB}) = {} & -10\log\left(l_b(R_t, h)\right) - 10\log\left(l_b(\rho - R_t, h)\right) \\ & + 10\log(\sigma_r) + 10\log(C). \end{aligned} \tag{5}$$

From (1) and (5), it shows that the echoes of an aircraft are the function of target RCS and propagation attenuation. The attenuation is related to the radar wavelength and the altitude of the target; it can be written as

$$l_b = 20\log\left|\frac{U_0}{U}\right|, \tag{6}$$

where U_0 is the Hertz vector and U is the Hertz vector of free space. In order to analyze the propagation attenuation of the ground wave, Rotheram attenuation model is utilized [14, 15].

When $d > 0.4\lambda^{1/3}a^{2/3}$ and $h_1 \le h_2 < \lambda^{2/3}a^{1/3}$, the Hertz vector can be defined as

$$U = \frac{\exp(-jkdm_0)}{\sqrt{ad\sin(d/a)}}\left(w_d + w_w + w_g\right), \tag{7}$$

where a is the Earth's radius and h_1 and h_2 are the antenna's height and target altitude, respectively. m_0 is the modified refractive index of the ground. w_d represents the direct wave, w_w is the reflected wave in the limit $\Delta \to \infty$, and Δ denotes the normalized surface impedance. w_g represents the combined reflected and surface waves.

Under the conditions that $d > 0.4\lambda^{1/3}a^{2/3}$ and $h_1 \le h_2 < \lambda^{2/3}a^{1/3}$, the Hertz vector is expressed as

$$\begin{aligned} U = {} & \sqrt{\frac{8\pi k^3 \exp(-j\pi/2)}{a\sin(d/a)}} \\ & \times \sum \frac{\exp(-jkdS_n)}{\Psi^{(2)}(S_n, 0)} \frac{g^{(2)}(S_n, H_1)}{g^{(2)}(S_n, 0)} \frac{g^{(2)}(S_n, H_2)}{g^{(2)}(S_n, 0)}, \end{aligned} \tag{8}$$

where the quantity $\Psi^{(2)}(S_n, 0)$ is the excitation factor for the nth mode. $g^{(2)}(S, H)$ is defined as the outgoing-wave height-gain function. H_1 and H_2 are the modified height of h_1 and h_2, respectively.

If the target altitude is high, the Hertz vector is computed with geometrical-optics formulas; it is computed as

$$\begin{aligned} U &= U_1 + U_3, \qquad d \le d_t, \\ U &= U_2 + U_3, \qquad d > d_t, \end{aligned} \tag{9}$$

where d_t is the transformation distance in which $U_1 = U_2$. U_1 is the direct ray when $d \le d_t$, U_2 represents the direct ray with $d > d_t$, and U_3 is defined as the reflected ray.

The relations between propagation attenuation and different target altitudes are illustrated in Figure 1, in which the radar frequency is 14 MHz. The target altitude varies from 0.5 km to 3 km and the range is changing from 50 km to 140 km.

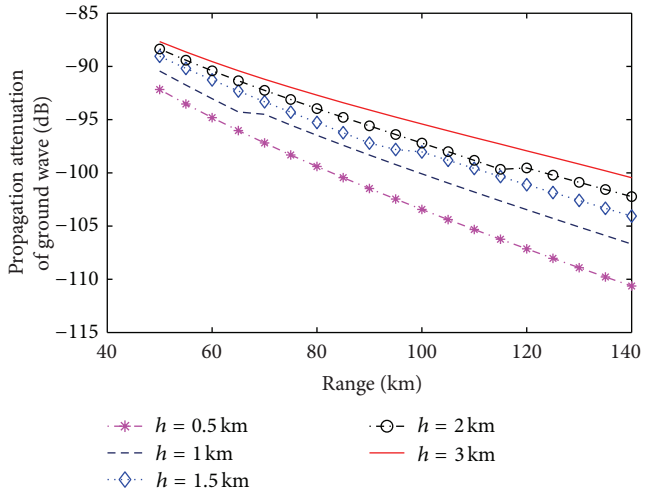

FIGURE 1: Propagation attenuation with different altitude.

The propagation attenuation in Figure 1 is computed by Rotheram attenuation model, which includes the effect of the atmospheric refraction. From Figure 1, it demonstrates that the propagation attenuation varies depending on target altitude, and there will be large propagation attenuation when the aircraft is low flying. While the altitude increases, the attenuation is weakened. As the propagation attenuation is the function of the range and altitude of the aircraft, therefore, the target echo amplitude is also relevant to target altitude and RCS. The radar would receive a more weakened echo when the aircraft is low flying. With these aforementioned properties, a simultaneous RCS and altitude estimation model is ready to be constructed in bistatic T/R-R HFSWR.

3. Simultaneous Altitude and RCS Fusion Estimation Model

In this section, a novel model would be established to estimate the target altitude and RCS. The state vector is defined as

$$\mathbf{X}(k) = \left[x(k), v_x(k), y(k), v_y(k), z(k), v_z(k), \sigma_t(k), v_{\sigma_t}(k), \sigma_r(k), v_{\sigma_r}(k)\right]^T, \tag{10}$$

where $x(k)$, $y(k)$, and $z(k)$ are the target positions along x, y, and z directions at time k. $v_x(k)$, $v_y(k)$ and $v_z(k)$ represent the velocities in three directions, respectively. $\sigma_t(k)$ and $\sigma_r(k)$, are the target RCS corresponding to the T/R and R stations at time k; the rates of change of RCS are denoted as $v_{\sigma_t}(k)$ and $v_{\sigma_r}(k)$, respectively.

The state equation is given by

$$\mathbf{X}(k) = \mathbf{F}\mathbf{X}(k-1) + \mathbf{v}(k-1), \tag{11}$$

where $\mathbf{F} \in \mathbf{R}^{10\times10}$ is the state transition matrix. $\mathbf{v}(k-1)$ represents the zero mean Gaussian random process noise with known covariance $\mathbf{Q}(k-1)$. In order to improve the estimation accuracy, four measurement vectors are established:

$$\begin{aligned}
\mathbf{Z}_1(k) &= \left[R_t(k), \rho(k), \theta_t(k), P_{tr}, P_{rr}\right]^T,\\
\mathbf{Z}_2(k) &= \left[R_t(k), \rho(k), \theta_r(k), P_{tr}, P_{rr}\right]^T,\\
\mathbf{Z}_3(k) &= \left[R_t(k), \theta_r(k), \theta_t(k), P_{tr}, P_{rr}\right]^T,\\
\mathbf{Z}_4(k) &= \left[\rho(k), \theta_r(k), \theta_t(k), P_{tr}, P_{rr}\right]^T.
\end{aligned} \tag{12}$$

It demonstrates that the target echoes information is incorporated into the measurements. The abovementioned four measurements are the nonlinear functions of state $\mathbf{X}(k)$. The measurement equation for each measurement vector can be modeled as

$$\mathbf{Z}_i(k) = h_i(\mathbf{X}(k)) + \mathbf{w}_i(k), \tag{13}$$

where $h_i(\cdot)$ denotes the nonlinear measurement function. Consider that $\mathbf{w}_i(k)$, $i = 1, 2, 3, 4$ are assumed to be mutually independent zero mean Gaussian random noises with known covariance $\mathbf{R}_i(k)$. That means that

$$E\left[\mathbf{w}_i(k)\mathbf{w}_j^T(k)\right] = 0, \quad i \neq j, i, \ j = 1, 2, 3, 4. \tag{14}$$

The range and azimuth information can be expressed as the functions of the state. They are denoted as

$$\begin{aligned}
R_t(k) &= \sqrt{(x(k)-x_t)^2 + (y(k)-y_t)^2 + (z(k)-z_t)^2},\\
\rho(k) &= \sqrt{(x(k)-x_r)^2 + (y(k)-y_r)^2 + (z(k)-z_r)^2}\\
&\quad + R_t(k),\\
\theta_r(k) &= \arctan\left(\frac{y(k)-y_r}{x(k)-x_r}\right),\\
\theta_t(k) &= \arctan\left(\frac{y(k)-y_t}{x(k)-x_t}\right),
\end{aligned} \tag{15}$$

where (x_t, y_t, z_t) and (x_r, y_r, z_r) are the locations of T/R and R stations. $\theta_t(k)$ and $\theta_r(k)$ represent the azimuths corresponding to T/R and R stations, respectively. For each measurement vector, (11) and (13) define the estimation model of target altitude and RCS.

An appropriate fusion of four measurements can contribute to higher accuracy of estimation; therefore, the centralized extended Kalman filter estimator is adopted to fuse four measurements. The fused state can be expressed as

$$\widehat{\mathbf{X}}(k,k) = \widehat{\mathbf{X}}(k,k-1) + \sum_{i=1}^{N}\mathbf{K}_i\left[\mathbf{Z}_i(k) - h_i\left(\widehat{\mathbf{X}}(k,k-1)\right)\right], \tag{16}$$

where N is the number of measurement vectors and $\mathbf{K}_i$ denotes the filter gain of ith measurement vector. The sate prediction at time k is written as

$$\widehat{\mathbf{X}}(k,k-1) = \mathbf{F}\widehat{\mathbf{X}}(k-1,k-1). \tag{17}$$

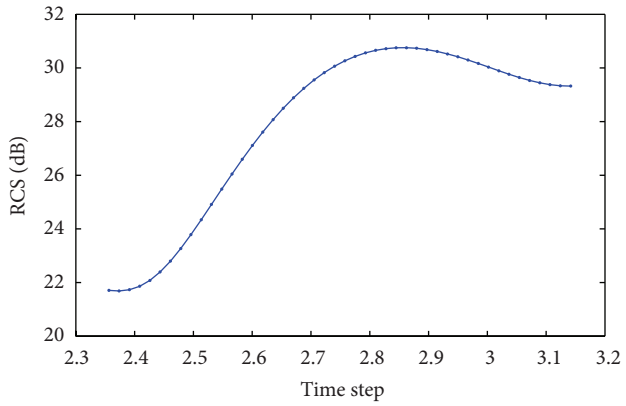

Figure 2: The RCS value at different attitude angle.

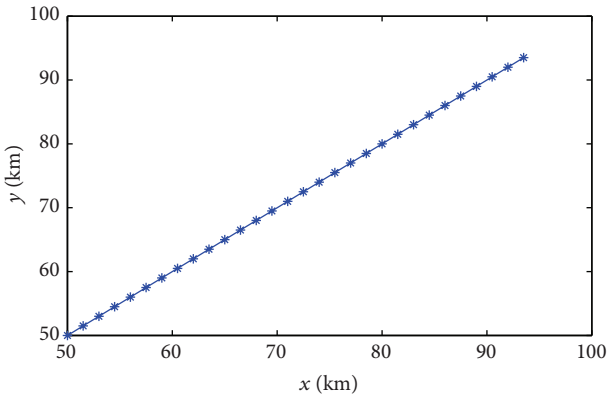

Figure 3: Flight trajectory in x-y plane.

The updated state covariance can be expressed as

$$\mathbf{P}^{-1}(k,k) = \mathbf{P}^{-1}(k,k-1) + \sum_{i=1}^{N} \left[\mathbf{P}_i^{-1}(k,k) - \mathbf{P}_i^{-1}(k,k-1)\right], \tag{18}$$

$$\mathbf{P}_i^{-1}(k,k) = \mathbf{P}_i^{-1}(k,k-1) + \mathbf{H}_i(k)^T \mathbf{R}_i(k)^{-1} \mathbf{H}_i(k), \tag{19}$$

$$\mathbf{P}(k,k-1) = \mathbf{F}\mathbf{P}(k-1,k-1)\mathbf{F}^T + \mathbf{Q}(k-1), \tag{20}$$

$$\mathbf{P}_i(k,k-1) = \mathbf{F}\mathbf{P}_i(k-1,k-1)\mathbf{F}^T + \mathbf{Q}(k-1), \tag{21}$$

where $\mathbf{P}_i(k,k)$ and $\mathbf{P}_i(k,k-1)$ are the updated sate covariance and prediction covariance associated with ith measurement vector, respectively.

4. Simulations

In order to evaluate the performance of the proposed model, a dynamic scenario is assumed. The T/R and R stations are located at (0, 0, 0) and (50 km, 0, 0), respectively. The initial position of the aircraft in x-y plane is (50 km, 50 km); flight altitude is defined as 7 km, 8.5 km, and 10 km, respectively. The velocities of the aircraft in x, y, and z directions are 150 m/s, 150 m/s, and 0 m/s. T = 10 s represents the time interval of measurement sampling. During the observation period, we assume the airplane of interest to be S27, which is simulated by FEKO software. In the flight scenario, the aircraft is flying away from the T/R station. As the attitude angle corresponding to T/R station is nearly a constant, the RCS is assumed to be 23 dB for simplicity. A Gaussian noise will be added in the state equation to model the fluctuation of the RCS. The RCS corresponding to R station changes at different attitude angles (a Gaussian noise will also be added to the state equation to model the fluctuation of RCS); it is presented in Figure 2.

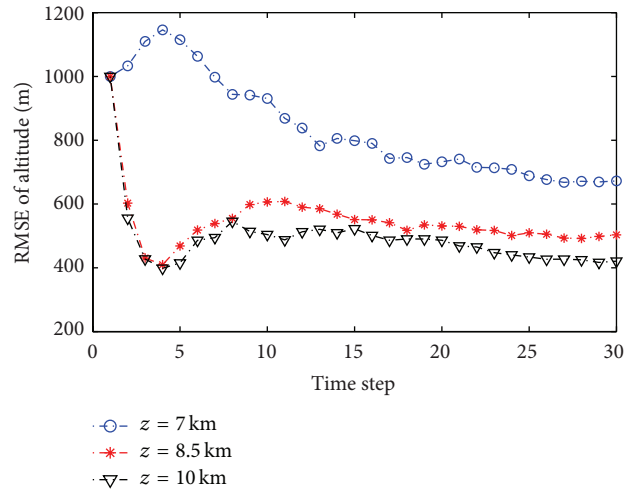

Figure 4: RMSE of altitude.

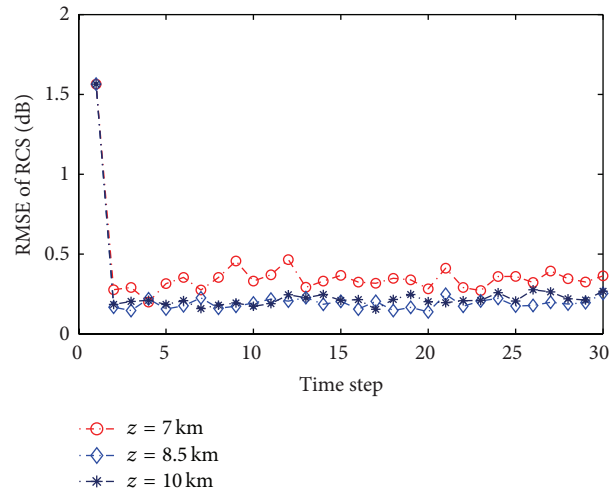

Figure 5: RMSE of RCS corresponding to the T/R station.

The variances of target range and azimuth are defined to be 500 m and 1°. The flight trajectory in x-y plane is denoted in Figure 3.

The root mean squared errors (RMSE) of the target altitude is depicted in Figure 4. RCS corresponding to the T/R and R stations are displayed in Figures 5 and 6.

In Figure 4, it demonstrates that the proposed method can estimate the altitude of aircraft with high accuracy. The

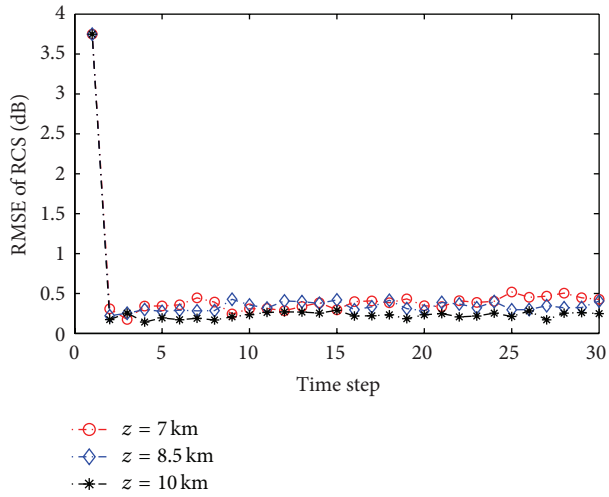

Figure 6: RMSE of RCS corresponding to the R station.

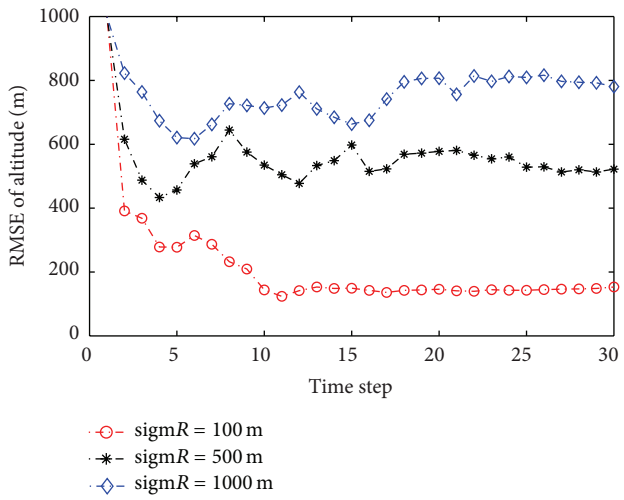

Figure 7: RMSE of altitude at different range errors.

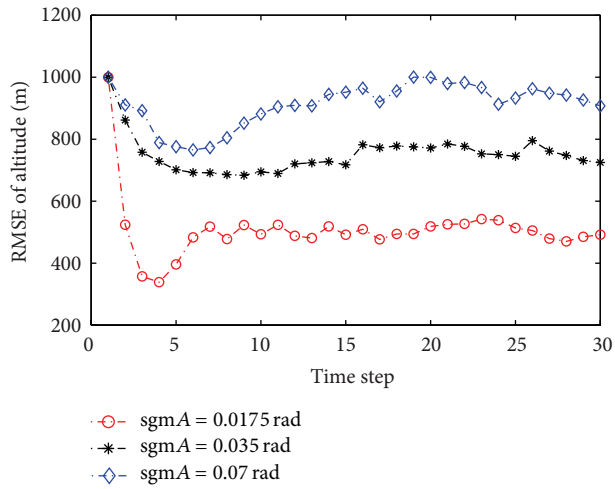

Figure 8: RMSE of altitude at different azimuth errors.

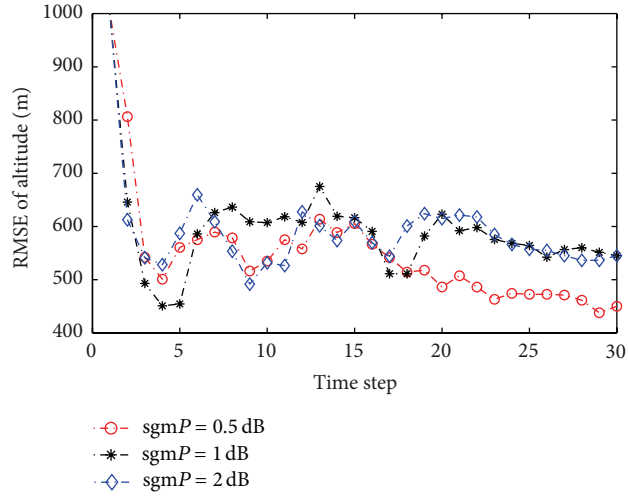

Figure 9: RMSE of altitude at different errors of echo amplitude.

RMSE of the altitude could converge to less than 700 m within 15 measurement intervals. The RMSE of altitude would have a significant decrement when target altitude increases; the reason is that posteriori Cramer-Rao lower bound (CRLB) on altitude is smaller at higher altitude. The estimator also provides preferable results of RCS estimation; RMSE of the RCS is less than 0.5 dB. The results in Figures 5 and 6 also show that there would be a smaller RMSE of RCS when target altitude increases, but it does not present a great improvement. It is that when the flying altitude becomes higher, ground wave attenuation is close to the atmospheric propagation attenuation gradually, the attenuation arising from seawater gets vanished, which leads to lower resolution of attenuation at high altitude.

The measurement errors have a great impact on the accuracy of the altitude estimation. The RMSE of altitude at three different measurement errors of range is presented in Figure 7; the range error is denoted as sig$R$. Figures 8 and 9 demonstrate the impact of azimuth and echo amplitude errors on altitude estimation. sig$A$ represents the azimuth error, and sig$P$ is the error of echo amplitude.

In Figures 7 and 8, it concludes that the range and azimuth errors perform a considerable impact on accuracy of altitude estimation. The results are deteriorating with the growth of range and azimuth errors. However, the accuracy of altitude is nearly invariable under three different errors of echo amplitude, which is depicted in Figure 9. The reason is that target range and azimuth information are sufficient to the altitude estimation, for which the echo amplitude information is redundant. Though the echo amplitude does not have remarkable impact on the estimation accuracy of altitude, it is essential for the RCS estimation. Inaccurate echo amplitude would result in a large estimation error of RCS. Figure 10 demonstrates the relationship between RMSE of RCS and different errors of echo amplitude.

In order to demonstrate the effectiveness of the proposed method, the altitude and RCS estimation results are showed compared with the traditional method [11], which

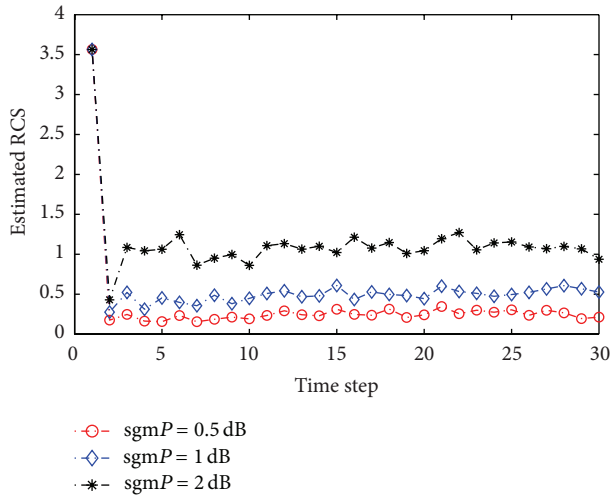

Figure 10: RMSE of RCS corresponding to T/R station at different errors of echo amplitude.

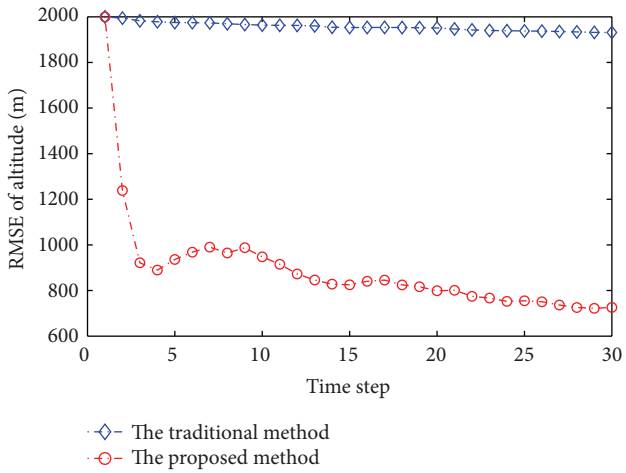

Figure 11: RMSE results of altitude between the traditional method and the proposed method.

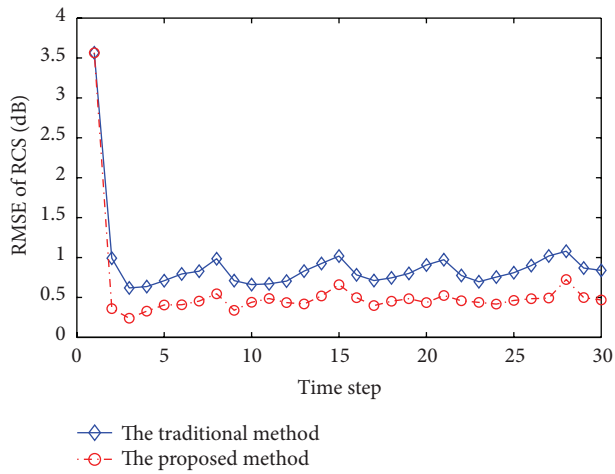

Figure 12: RMSE results of RCS between the traditional method and the proposed method.

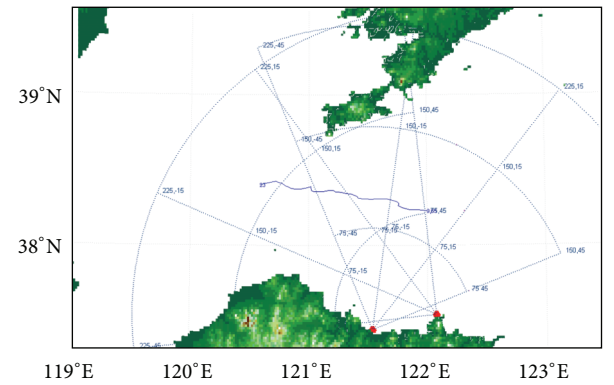

Figure 13: Flight trajectory of an unknown civil airplane in T/R-R HFSWR.

are depicted in Figures 11 and 12. In the simulations, the airplane is assumed to be flying at an altitude of 10 km, and the variances of target range and echo amplitude are 500 m and 0.5 dB, respectively.

From the altitude results of Figure 11, it shows that the proposed method outperforms the traditional method. The RMSE of the altitude keeps nearly a constant, which cannot converge to a considerable result. However, the proposed method provides preferable altitude estimation under the circumstances of large initialization errors. It is that the proposed model is completely observable to the altitude and RCS information, which is lacked in the traditional model. The traditional method presents an impressive estimation of RCS, as depicted in Figure 12. It does not demonstrate the good performance of the traditional method. The reason is that when the target is high flying, ground wave attenuation is close to the atmospheric propagation attenuation gradually. The attenuation arising from seawater gets vanished, which leads to lower resolution of attenuation at high altitude.

In the following section, a practical example is used to make further evaluations of the proposed model. A scenario of international airplane is presented in Figure 13, in which the airplane is an uncooperative target. The radar frequency of operation is 8.9 MHz; the range between T/R and R station is 54.3 km.

The altitude and RCS estimation results are depicted from Figures 14, 15, and 16.

From Figures 14 to 16, it is shown that the proposed model provides considerable altitude and RCS estimation. The altitude is estimated to be 9.5 km. Although the ground truth is unknown, this estimation result is acceptable for an international airplane, which flies approximately at 10 km of altitude, and the effectiveness of the presented model is verified.

The simulations and practical examples demonstrate that the new method provides significant improvements compared with the traditional method. It results from the complete observability of the proposed model. The altitude and RCS information of the target can be estimated with

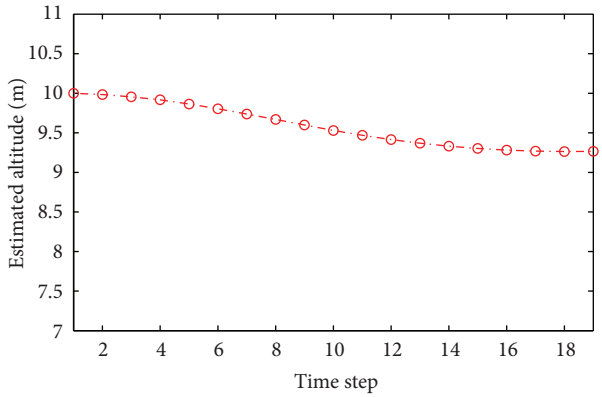

FIGURE 14: The estimated altitude of an international flight.

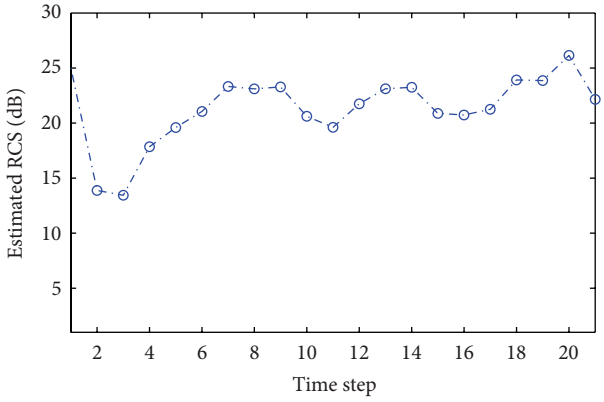

FIGURE 15: The estimated RCS corresponding to T/R station.

high accuracy. Even the errors of initial target state are large; the results of the fusion model converge quickly within a few measurements. Although the proposed method presents an impressive performance, the flaw is that it demands that the airplane should be detected by the T/R and R stations simultaneously. When the target is detected by only one receiver, the fusion approach could not be performed. Under such circumstances, an accurate estimation result could not be guaranteed.

5. Conclusions

A simultaneous altitude and RCS estimator is proposed with the propagation attenuation in bistatic HFSWR. It utilizes the variation property of propagation attenuation at different altitudes. In order to improve the accuracy of estimation, four measurement vectors are constructed with range, azimuth, and echo amplitude; centralized optimal fusion is adopted to fuse the measurements. Simulations and a practical example show that the proposed model provides preferable results of estimation with small RMSE, which demonstrates the benefits from using this altitude and RCS estimator.

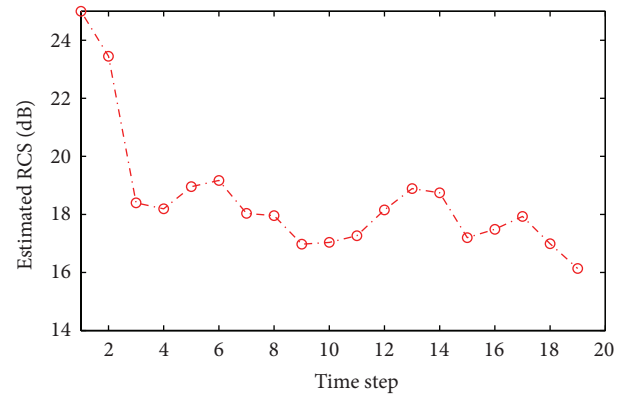

FIGURE 16: The estimated RCS corresponding to R station.

Acknowledgment

This work was supported by the National Natural Science Foundation of China under Grant no. 61171188.

References

[1] G. Rujiang, Y. Yeshu, and Q. Taifan, "Adaptive modified hough transform track initiator for HFSWR tracking of fast and small targets," *Journal of Systems Engineering and Electronics*, vol. 16, no. 2, pp. 316–320, 2005.

[2] G. Fabrizio, F. Colone, P. Lombardo, and A. Farina, "Adaptive beamforming for high-frequency over-the-horizon passive radar," *IET Radar, Sonar and Navigation*, vol. 3, no. 4, pp. 384–405, 2009.

[3] W. Huang, E. Gill, X. Wu, and L. Li, "Measurement of sea surface wind direction using bistatic high-frequency radar," *IEEE Transactions on Geoscience and Remote Sensing*, vol. 50, no. 10, pp. 4117–4122, 2012.

[4] S. J. Anderson, "Optimizing HF Radar Siting for surveillance and remote sensing in the strait of Malacca," *IEEE Transactions on Geoscience and Remote Sensing*, vol. 51, no. 3, pp. 1805–1816, 2013.

[5] L. Bruno, P. Braca, J. Horstmann, and M. Vespe, "Experimental evaluation of the Range-Doppler coupling on HF surface wave radars," *IEEE Geoscience and Remote Sensing Letters*, vol. 10, no. 4, pp. 850–854, 2013.

[6] Z. Hao and W. Biyang, "Radio frequency interference suppression in small-aperture high-frequency radars," *IEEE Geoscience and Remote Sensing Letters*, vol. 9, no. 4, pp. 788–792, 2012.

[7] Z. Zhao, X. Wang, and Q. Shao, "Multipath clutter rejection for digital radio mondiale-based HF passive bistatic radar with OFDM waveform," *IET Radar Sonar and Navigation*, vol. 6, no. 9, pp. 867–872, 2013.

[8] W. Wang and L. R. Wyatt, "Radio frequency interference cancellation for sea-state remote sensing by high-frequency radar," *IET Radar, Sonar and Navigation*, vol. 5, no. 4, pp. 405–415, 2011.

[9] M. J. Gai and Y. I. Xiao, "An approach to tracking a 3D target with 2D radar," in *Proceedings of the IEEE International Radar Conference*, pp. 763–768, Arlington, UK, 2005.

[10] Z. Kongrui, Z. Gongjian, Y. Changjun, and Q. Taifan, "Altiude estimation in high frequencysurface wave radar," unpublished.

[11] P. E. Howland and C. F. Clutterbuck, "Estimation of target altitude in HF surface wave radar," in *Proceedings of the 7th International Conference on HF Radio Systems and Techniques*, pp. 296–300, July 1997.

[12] Y. He, G. Wang, J. Xiu, and H. Yan, "Combinatorial estimation and location accuracy analysis in bistatic/multistatic radars," *Chinese Journal of Electronics*, vol. 28, no. 3, pp. 17–20, 2000 (Chinese).

[13] Y. Lei, C.-B. Zhu, X.-X. Feng, and B.-B. Li, "Estimation of aircraft altitude in 2D radar intelligence networking," in *Proceedings of the 2nd International Conference on Signal Processing Systems (ICSPS '10)*, vol. 2, pp. V2331–V2333, Dalian, China, July 2010.

[14] S. Rotheram, "Ground-wave propagation. Part 1: theory for short distances," *IEE Communications Radar and Signal Processing*, vol. 128, no. 5, pp. 275–284, 1981.

[15] S. Rotheram, "Ground-wave propagation Part2: theory for short distances," *IEE Communications Radar and Signal Processing*, vol. 128, no. 5, pp. 285–295, 1981.